

Unprecedented plastic flow channel in γ -B₂₈ through ultrasoft bonds: A challenge to superhardness

HPSTAR
666-2018

S. H. Zhang,^{1,2} X. Zheng,³ Q. Q. Jin,⁴ S. J. Zheng,⁴ D. Legut,⁵ X. H. Yu,^{3,*} H. Y. Gou,⁶ Z. H. Fu,^{1,2} Y. Q. Guo,^{1,2}
B. M. Yan,⁶ C. Peng,⁶ C. Q. Jin,³ T. C. Germann,⁷ and R. F. Zhang^{1,2,*}

¹*School of Materials Science and Engineering, Beihang University, Beijing 100191, People's Republic of China*

²*Center for Integrated Computational Materials Engineering, International Research Institute for Multidisciplinary Science, Beihang University, Beijing 100191, People's Republic of China*

³*Beijing National Laboratory for Condensed Matter, Institute of Physics, Chinese Academy of Sciences, Beijing 100190, People's Republic of China*

⁴*Shenyang National Laboratory for Materials Science, Institute of Metal Research, Chinese Academy of Sciences, Shenyang 110016, China*

⁵*IT4Innovations Center, VSB-Technical University of Ostrava, CZ-70833 Ostrava, Czech Republic*

⁶*Center for High Pressure Science and Technology Advanced Research Room C208, No.10 Dongbeiwang West Road, Haidian, Beijing 100094, China*

⁷*Theoretical Division, Los Alamos National Laboratory, Los Alamos, New Mexico 87545, USA*



(Received 19 March 2018; revised manuscript received 9 August 2018; published 13 December 2018)

A longstanding controversy remains whether γ -B₂₈ is intrinsically superhard or not, i.e., $H_v \geq 40$ GPa. Here we perform comprehensive investigations on the mechanical properties of γ -B₂₈ to reveal the plasticity and failure mode of γ -B₂₈ through the unique combination of microindentation experiment, the ideal strength approach, and the *ab initio* informed Peierls-Nabarro model. A low load-invariant hardness of ~ 30 GPa is found for both polycrystalline and monocrystalline γ -B₂₈. By carefully checking the strength anisotropy and strain facilitated phonon instability, a surprising ideal strength of 23.1 GPa is revealed along the (001)[010] slip system for γ -B₂₈, together with an inferior Peierls stress of 3.2 GPa, both of which are close to those of B₆O and ZrB₁₂ yet much lower than those of diamond and c-BN. These results suggest that γ -B₂₈ could not be intrinsically superhard. Atomistic simulation and electronic structure analysis uncover an unprecedented plastic flow channel through the specific ultrasoft bonding, which causes a dramatic softening of γ -B₂₈. These findings highlight an approach to quantifying the realistic hardness by means of two plasticity descriptors beyond the elastic limit, i.e., the ideal strength approach and the Peierls-Nabarro model.

DOI: [10.1103/PhysRevMaterials.2.123602](https://doi.org/10.1103/PhysRevMaterials.2.123602)

Superhard materials have always been an important research topic because of their fundamental importance in material science/physics and technological applications such as cutting and polishing tools in the machinery industry and drilling bits in the milling and petrochemical industry [1–3]. With the threshold of load-invariant Vickers hardness higher than 40 GPa, only diamond and c-BN can be qualified as intrinsically superhard materials unambiguously so far. Unfortunately, each of these shows some inherent shortcomings, such as the inferior thermal stability for diamond [4] and the extreme synthesis condition for c-BN [1]. In the search for new superhard materials, one of the polymorphs of elemental boron, γ -B₂₈, has been claimed as the second hardest elemental solid after diamond with Vickers hardness ≥ 50 GPa (e.g., 58 [5] and 50 GPa [6]), which was also thought to be consistent with the theoretically predicted hardness of γ -B₂₈, i.e., 42.5 and 49 GPa according to the Lyakhov and Oganov [7] and Chen *et al.* [8] hardness models, respectively. It seems that a consensus between experiment and theory has been approached regarding the superhardness of γ -B₂₈; however,

two recent fundamental contradictions have reignited scientific curiosity and general interest:

(i) The load-invariant hardness of well-synthesized polycrystalline γ -B₂₈ was only about 30.3 GPa [9].

(ii) The determined ideal shear strength of γ -B₂₈ (21.6 GPa [10]) is unexpectedly much lower than that of c-BN, even much lower than that of ZrB₁₂ (34.5 GPa [11]) and B₆O (38.0 GPa [12]).

Furthermore, it is recognized that a fundamental issue exists in the adopted hardness models for predicting γ -B₂₈ to be superhard, that is, the model parameters are generally derived from the equilibrium structure within the elastic limit, whereas the hardness of a real material is determined by the crystal plasticity [1]. These critical issues bring researchers to reconsider the longstanding controversy of whether the γ -B₂₈ is intrinsically superhard or not in view of its potential application and scientific interest [13–15], and to pursue what plasticity-relevant parameters can be used to provide a more realistic quantification on the intrinsic hardness of materials.

For this purpose, in the present paper, both polycrystalline and monocrystalline γ -B₂₈ samples were prepared by means of high-pressure and high-temperature experiments, and then their hardnesses were carefully determined and compared with other typical hard or superhard materials at the same

*Corresponding authors: yuxh@iphy.ac.cn;
huiyang.gou@hpstar.ac.cn; zrf@buaa.edu.cn

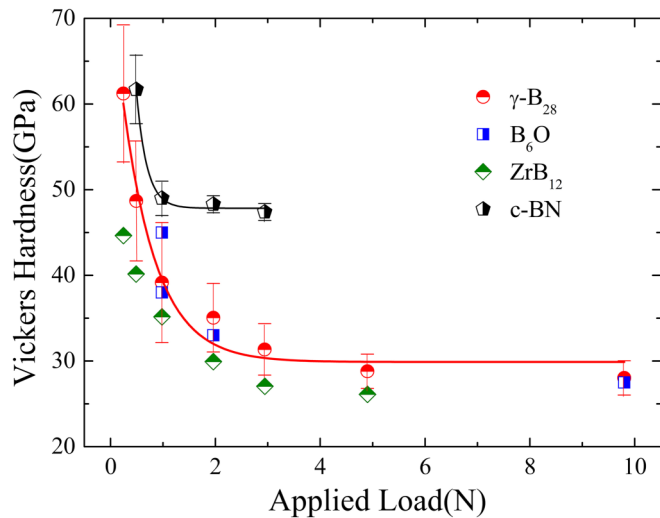


FIG. 1. The average measured H_v for polycrystalline γ -B₂₈ and c-BN under different loads. The measured H_v of B₆O [21–25] and ZrB₁₂ [11] under different loads are also shown for a global realistic comparison, including both the hardness values at low load and those until load invariance.

sufficiently high loading conditions. The results suggest that γ -B₂₈ could not be intrinsically superhard but has a low load-invariant hardness of ~ 30 GPa. On the other hand, two plasticity-relevant qualities, i.e., the ideal strength and the Peierls stress, were incorporated to explore the two plastic deformation mechanisms in hard and superhard materials at the atomic scale: (1) atomically sharp step induced bond rupture due to the lack of independent slip systems [16] and (2) dislocation networks surrounding the crack tip under indentation, which have been concluded to be a crucial role for extensive plasticity of brittle materials [16]. The former quality is determined by electronic instability of a perfect crystal under affine deformation with a large strain [17,18], while the latter one provides a quantitative lattice resistance to dislocation slip, which can be modeled by means of the Peierls-Nabarro (P-N) model [19,20]. Our calculated ideal

shear strength and Peierls stress provide consistent support of the experimental observations, and the atomistic mechanism underlines that both the lattice instability under affine deformation and the sliding under alias deformation are dominated by the ultrasoft bonds appearing between icosahedral boron nanocages.

Figure 1 shows the determined polycrystalline Vickers hardness (H_v) as a function of applied loads from 0.25 to 9.8 N. It is seen that γ -B₂₈ has a load-invariant hardness of 29 GPa at 9.8 N, which is similar to that of B₆O [21–25] and ZrB₁₂ [11] but much lower than that of c-BN (see Fig. 1). The measured H_v of γ -B₂₈ in our experiments is much lower than the previous results of 58 [5] and 50 GPa [6], but in good agreement with the experimental data of 30.3 GPa for polycrystalline γ -B₂₈ in Ref. [9]. The single crystalline γ -B₂₈ with grain sizes ranging from tens of micrometers to 100 micrometers was also prepared and its experimentally determined hardness is shown in Fig. S2 in the Supplemental Material [26]. Interestingly, with tens of indentation measurements on different planes of single-crystal grains from three batches of samples, the statistic hardness data of the anisotropic hardness range from 32 to 26 GPa under a 9.8-N loading, which is almost the same as that of the polycrystal sample and suggests a weakly anisotropic hardness behavior of γ -B₂₈. In the following, we will suggest theoretically, via the ideal strength model and P-N model, that γ -B₂₈ is intrinsically hard but not superhard, as determined experimentally in our paper.

Figure 2(a) shows the calculated stress-strain curves of γ -B₂₈ along the weakest tensile and shear paths via affine deformation considering both pure and simple shears; Fig. 2(b) presents the anisotropy of ideal shear strength of γ -B₂₈ on the (001) and \perp [011] planes [27] to identify the lowest shear strength via affine simple shear deformation. It reveals that the lowest shear strength (23.8 GPa) is indeed along the (001)[010] path, while on the \perp [011] plane the lowest shear strength of 25.9 GPa is observed along the direction of 30° or 150° deviating from the [100] direction. Furthermore, the phonon dispersion curve of the structure under shear strain of 0.1487 (at peak) along the weakest (001)[010] path was also investigated and compared with that of the unstrained

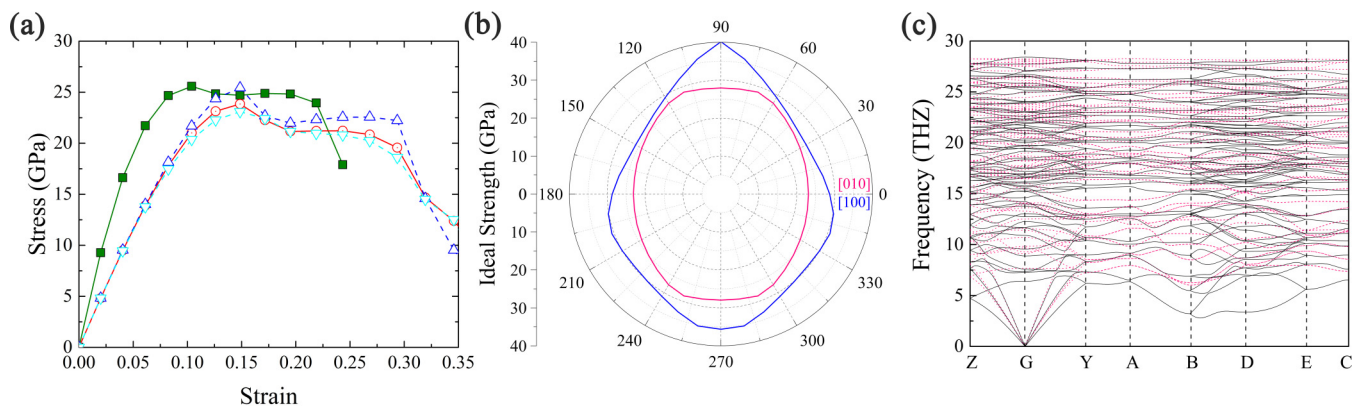


FIG. 2. (a) The calculated stress-strain curve of γ -B₂₈ along the weakest tensile (solid) and shear (open) paths via affine pure (solid line) and simple (dashed line) shear deformations. (b) The ideal shear strengths along different directions on the (001) (red) and \perp [011] (blue) planes. (c) Calculated phonon dispersion curves for the structures under strains of 0.000 (black solid line) and 0.1487 (red dashed line) along the (001)[010] slip system.

TABLE I. The minimum ideal tensile (σ_{\min}) and shear (τ_{\min}) strengths, the ideal cleavage stress σ_{IC} and ideal slide stress τ_{IS} , as well as the Peierls stress (τ_P) (in gigapascal). The properties of other typical hard and superhard covalent materials including diamond, c-BN, B₆O, ZrB₁₂, and Si are also listed for comparison. The experimental Vickers hardness (H_v) is listed in the last column (in gigapascal) together with the available load values used in the related experiments in brackets (in newton). The units of a'_{edge} and a'_{screw} are in angstrom.

Materials	σ_{\min}	τ_{\min}	σ_{IC}	Slip system	τ_{IS}	a'_{edge}	$\tau_{P,\text{edge}}$	a'_{screw}	$\tau_{P,\text{screw}}$	H_v
Diamond	83.4 ^a 82.3 [12]	87.1 ^a 86.8 [12]	100.6	(111)[1 $\bar{1}$ 0] ^b	125.1	1.26	13.0	2.19	60.7	96 ± 5 [35]
c-BN	56.3 ^a 55.3 [30]	59.6 ^a 58.3 [30]	94.0	(111)[1 $\bar{1}$ 0] ^b	89.2	1.28	10.3	2.22	44.0	47(3), ^c 63 ± 5 [35], 48 [36], 47(5) [22]
B ₆ O	53.8 ^a 53.3 [12]	37.9 ^a 38.0 [12]	56.4	(0001)[10 $\bar{1}$ 0]	51.2	4.67	7.9	2.70	3.1	33(2) [23,24], 27.5(10) [25]
γ -B ₂₈	25.6 ^a 25.3 [10]	23.8 ^a 21.6 [10]	46.8	(001)[010]	43.3	2.80	3.2	2.52	3.4	29.9(10), ^c 30.3(20) [9]
ZrB ₁₂	49.9 ^a 49.6 [11]	34.8 ^a 34.5 [11]	56.7	(111)[1 $\bar{1}$ 0] (111)[1 $\bar{1}$ 2]	55.2 55.3	2.62	2.2	4.53	22.4	27(5) [11]
Si	19.2 ^a 22.0 [31]	7.8 ^a 6.8 [31]	20.2	(111)[1 $\bar{1}$ 0] ^b	13.5	1.93	1.7 0.6–2.8 ^d [33]	3.35	6.9 3–4 [33], 6.2 [34]	

^aThe ideal strengths under affine pure shear deformation.

^bThe SFEs on the shuffle plane are used due to their lower values than those on the glide plane.

^cThe experimental hardness obtained in this paper.

^dThe Peierls stress of 60° dislocation on the shuffle plane.

structure [see Fig. 2(c)]. It is interestingly found that the phonon instability, that appears in Al [28] and Si [29] under strain, does not occur for γ -B₂₈ as the shear deformation is applied along the (001)[010] slip system. All in all, γ -B₂₈ has the lowest tensile strength of 25.6 GPa along the [011] direction, and the lowest shear strength of 23.8 GPa along the (001)[010] shear deformations, which are consistent with the previous results, i.e., 25.3 GPa for tension and 21.6 GPa for shear [10]. These values are only about 31 and 45% of those of diamond and c-BN for ideal tensile strength, and 27 and 40% of those of diamond and c-BN for ideal shear strength, respectively (see Table I [10–12,30,31]). Notably, the ideal shear strength of γ -B₂₈ is about 37 and 32% lower than that of B₆O and ZrB₁₂, respectively, indicating that γ -B₂₈ should be intrinsically weaker than B₆O and ZrB₁₂. Such a finding contradicts surprisingly that the experimentally determined hardness of γ -B₂₈ is slightly higher than that of ZrB₁₂ (see Fig. 1), and therefore promotes a critical argument on the scaling rule of hardness by ideal strength that was widely used in previous studies [10]. For this purpose, below, we shall introduce another plasticity parameter, i.e., Peierls stress, to provide a realistic explanation of the physical origin of such inconsistency.

By comparing the calculated ideal strengths via affine deformation, one can determine the weakest link in a perfect crystal, which corresponds to the cleavage or sliding plane where fracture occurs or dislocation resides. To account for the fracture of dislocation mediated crystal plasticity, alias deformation, i.e., only one layer of the crystal displaced along the tensile or shear direction, is more relevant since the localized deformation governs the inhomogeneous fracture or plastic deformation in a crystal. Therefore, the ideal cleavage and slide stresses by alias deformation are further explored to see if they may explain the comparable hardnesses between γ -B₂₈, B₆O and ZrB₁₂. Figure 3(a) shows the

calculated cleavage energy $E_b(d)$ [32] and associated stress $\sigma(d) \equiv \partial E_b / \partial d$ versus cleavage opening d normal to the (001) plane of γ -B₂₈. It is found in Table I that the ideal cleavage stress $\sigma_{\text{IC}} \equiv \max\{\sigma(d)\}$ of γ -B₂₈ is 46.8 GPa, which is lower than that of B₆O (56.4 GPa) and ZrB₁₂ (56.7 GPa), suggesting that γ -B₂₈ is more brittle and has a lower interplanar cleavage resistance as compared to B₆O and ZrB₁₂.

To account for the dislocation mediated plastic resistance, the stacking fault energy (SFE) profile of γ -B₂₈ versus displacement (u/b) for the (001)[010] slip system is determined by alias shear deformation, and presented in Fig. 3(b). By incorporating the SFE profile into the P-N model, the corresponding disregistry $u(x)$ and misfit density $\rho(x)$ of edge dislocation are obtained and shown in Fig. 3(c). It is found that the perfect dislocation separates two partials with a strong interaction between them, attributed by the appearance of stable SFE along the (001)[010] slip system. In an illustrative atomic-scale representation, Fig. 3(d) presents the pressure field around dislocation cores as defined in Ref. [20]. It is also clearly observed that two partial dislocations (denoted by “L”) are separated by a planar stacking fault in between. The results of the P-N model along the weakest shear path, including the ideal slide stress $\tau_{\text{IS}} = \max\{\tau(u)\}$ as well as the Peierls stress (τ_P) for both edge and screw dislocations, are summarized in Table I together with the previous theoretical values [33,34] for comparison. It is found that both the ideal slide stress (43.3 GPa) and Peierls stress (3.2 GPa) of γ -B₂₈ are much smaller than those of diamond (125.1 and 13.0 GPa) and c-BN (89.2 and 10.3 GPa), in agreement with the conclusion drawn from the calculated ideal strength via affine deformation. It is, however, unexpectedly noticed that, although the ideal slide stress of γ -B₂₈ (43.3 GPa) is lower than that of B₆O (51.2 GPa) and ZrB₁₂ (55.2 GPa), γ -B₂₈ has a nearly identical Peierls stress with that of B₆O (3.1 GPa), both of which are larger than that of ZrB₁₂ (2.2 GPa).

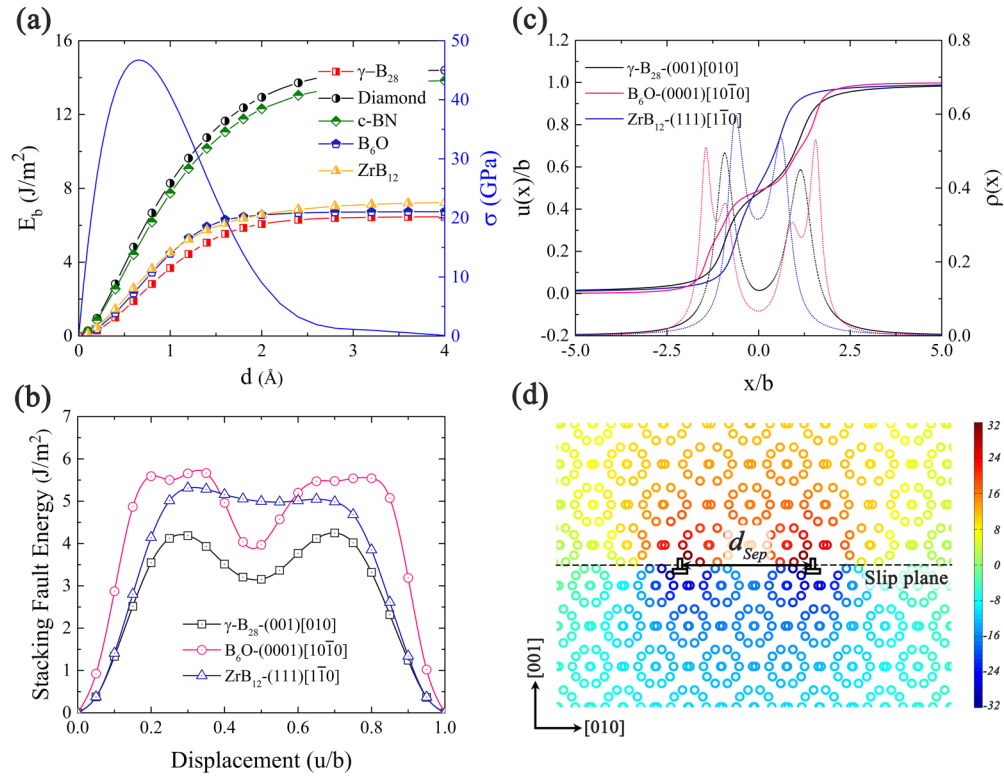


FIG. 3. (a) Cleavage energy $E_b(d)$ vs cleavage opening d for the γ -B₂₈-(001) plane together with those of diamond-(111), c-BN-(111), B₆O-(0001), and ZrB₁₂-(111) planes for comparison. Only the associated stress $\sigma(d) \equiv \partial E_b / \partial d$ of γ -B₂₈ is shown with a solid line. (b) The SFE profile vs displacement (u/b) and (c) the disregistry $u(x)$ and misfit density $\rho(x)$ of edge dislocation for the (001)[010] slip system. The SFE profiles and dislocation core structures of B₆O-(0001)[10 $\bar{1}$ 0] and ZrB₁₂-(111)[1 $\bar{1}$ 0] slip systems are also shown for comparison. (d) The pressure field (in gigapascal) around the dislocation core of the γ -B₂₈-(001)[010] slip system as defined in Ref. [20].

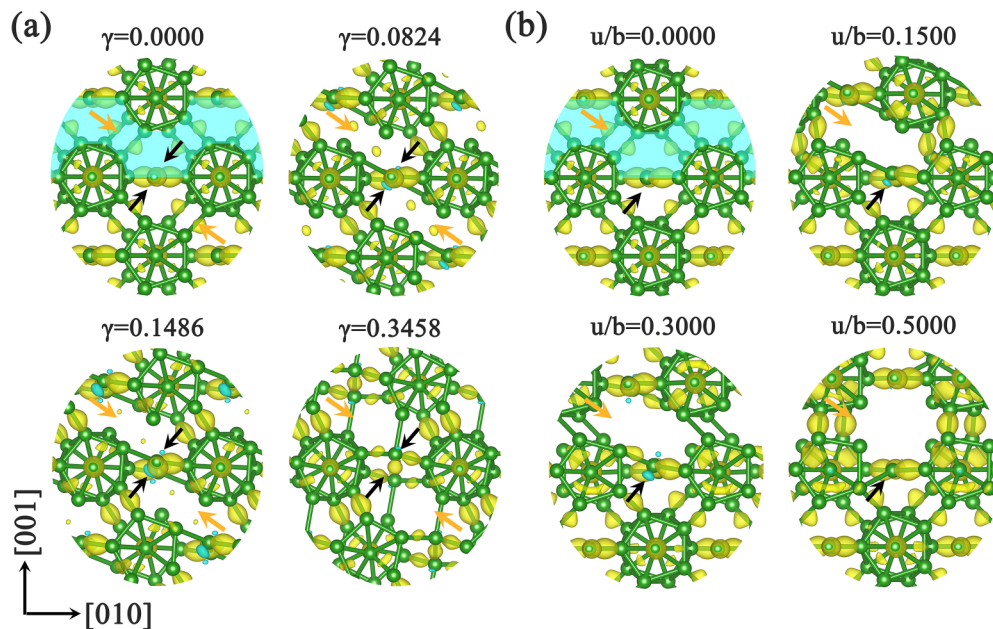


FIG. 4. Isosurfaces of the VCDD of γ -B₂₈ under (a) affine simple shear deformation with different strains $\gamma = 0.0000, 0.0824, 0.1486$ (at peak), and 0.3458 (after lattice instability) and (b) alias shear deformation with different displacements $u/b = 0.0000, 0.1500, 0.3000$ (at unstable SFE), and 0.5000 (at stable SFE) along the (001)[010] slip system. A same isosurface level of $\pm 0.022 e/\text{bohr}^3$ is used in these plots. The plastic flow channel through ultrasoft bonds is illustrated as the cyan area.

Based on the aforementioned discussions, it is undoubtedly concluded that the hardness of γ -B₂₈ must be much lower than that of diamond and c-BN due to its much lower ideal strengths of both affine and alias deformations as well as the Peierls stress, which agrees with that the experimental Vickers hardness of diamond ($H_v = 96$ GPa [35]) and c-BN ($H_v = 47$ – 63 GPa [22,35,36]) versus that of γ -B₂₈ ($H_v = 29$ GPa in this paper). In addition, due to its larger Peierls stress, γ -B₂₈ has a slightly larger hardness than that of ZrB₁₂ (see Fig. 1), though the ideal strengths of ZrB₁₂ are much greater than those of γ -B₂₈. Meanwhile, due to the nearly equal Peierls stress but a lower ideal strength, the hardness of γ -B₂₈ is close to that of B₆O under large load (e.g., 35 versus 33 GPa [21–25] at a load of 1.98 N and 29 versus 28 GPa at a load of 9.8 N as shown in Fig. 1). This illustrates why γ -B₂₈ with a lower ideal strength could be harder than ZrB₁₂. It is also confirmed that γ -B₂₈ is not intrinsically superhard by the previous experimental results of 58 [5] and 50 GPa [6], but has a low hardness of ~ 30 GPa obtained in our experimental work, providing a consistency between theoretical analysis and experimental observation.

To gain an in-depth insight into the electronic origin of the low hardness and strength of γ -B₂₈, the variations of valence charge density difference (VCDD) of γ -B₂₈ under affine and alias deformations along the (001)[010] slip system are presented in Fig. 4. It is found surprisingly that the ultrasoft bonds, which connect the icosahedral B₁₂ clusters (highlighted by orange arrows), provide a plastic flow channel in γ -B₂₈ (see the cyan area in Fig. 4), along which a much lower Peierls stress is found for dislocation mobility than that of diamond and c-BN. Moreover, a new stable state is reached as the charge depletion regions disappear, and consequently a new configuration of B₂ dumbbell pairs forms, as highlighted by black arrows in Fig. 4(a), which causes an anomalously large creeplike plasticity of γ -B₂₈ along the (001)[010] slip system [10]. In a similar manner to affine deformation, a plastic flow channel is also observed under alias shear deformation [see Fig. 4(b)], and also when the

charge depletion regions disappear the initial configuration of B₂ dumbbell pairs will recover, resulting in the formation of stable SFE at $u/b = 0.5000$.

In summary, we have performed comprehensive investigations on the mechanical properties of γ -B₂₈ to identify different failure (plasticity) modes of γ -B₂₈ through the synergic techniques of microindentation experiment, the ideal strength approach, and the *ab initio* informed Peierls-Nabarro model. It is found that γ -B₂₈ has an ideal strength of 23.8 GPa along the (001)[010] slip system, together with an inferior Peierls stress of 3.2 GPa, both of which are close to those of B₆O and ZrB₁₂ yet much lower than those of diamond and c-BN. All of these results confirm that γ -B₂₈ is not intrinsically superhard, but has a low asymptotic hardness of ~ 30 GPa, as determined experimentally in our paper. Electronic structure calculations suggest that a plastic flow channel in γ -B₂₈ is accomplished through ultrasoft bonds, limiting it to be superhard. These findings highlight that a combined analysis of the ideal strength and Peierls stress provides a unique quantification on the hardness of materials compared with the widely used hardness model and elastic moduli, because of their direct plasticity relevancy.

This work is supported by the National Natural Science Foundation of China (Grants No. 51672015, No. 51201148, and No. U1530402), National Key Research and Development Program of China (Grant No. 2016YFC1102500), National Thousand Young Talents Program of China, and Fundamental Research Funds for the Central Universities. D.L. was supported by project IT4Innovations: Path to Exascale (Grant No. CZ.02.1.01/0.0/0.0/16_013/0001791), Czech Science Foundation (Grant No. 17-27790S), and National Programme of Sustainability (Grant No. LQ1602). X.H.Y. was supported by the National Key R&D Program of China (Grant No. 2016YFA0401503), and the National Natural Science Foundation of China (Grants No. 11575288 and No. 51402350).

S.H.Z., X.Z., and Q.Q.J. contributed equally to this work.

-
- [1] R. B. Kaner, J. J. Gilman, and S. H. Tolbert, *Science* **308**, 1268 (2005).
- [2] S. Veprek, *J. Vac. Sci. Technol. A* **31**, 050822 (2013).
- [3] T. Irifune, A. Kurio, S. Sakamoto, T. Inoue, and H. Sumiya, *Nature (London)* **421**, 599 (2003).
- [4] J. E. Westraadt, I. Sigalas, and J. H. Neethling, *Int. J. Refract. Met. Hard Mat.* **48**, 286 (2015).
- [5] E. Y. Zarechnaya, L. Dubrovinsky, N. Dubrovinskaia, Y. Filinchuk, D. Chernyshov, V. Dmitriev, N. Miyajima, A. El Goresy, H. F. Braun, S. Van Smaalen, I. Kantor, A. Kantor, V. Prakapenka, M. Hanfland, A. S. Mikhaylushkin, I. A. Abrikosov, and S. I. Simak, *Phys. Rev. Lett.* **102**, 185501 (2009).
- [6] V. L. Solozhenko, O. O. Kurakevych, and A. R. Oganov, *J. Superhard Mater.* **30**, 428 (2008).
- [7] A. O. Lyakhov and A. R. Oganov, *Phys. Rev. B* **84**, 092103 (2011).
- [8] X. Q. Chen, H. Y. Niu, D. Z. Li, and Y. Y. Li, *Intermetallics* **19**, 1275 (2011).
- [9] J. Q. Qin, N. Nishiyama, H. Ohfujii, T. Shinmei, L. Lei, D. W. He, and T. Irifune, *Scr. Mater.* **67**, 257 (2012).
- [10] W. Zhou, H. Sun, and C. F. Chen, *Phys. Rev. Lett.* **105**, 215503 (2010).
- [11] T. Ma, H. Li, X. Zheng, S. M. Wang, X. C. Wang, H. Z. Zhao, S. B. Han, J. Liu, R. F. Zhang, and P. W. Zhu, *Adv. Mater.* **29**, 1604003 (2017).
- [12] R. F. Zhang, Z. J. Lin, Y. S. Zhao, and S. Veprek, *Phys. Rev. B* **83**, 092101 (2011).
- [13] M. I. Eremets, V. V. Struzhkin, H. Mao, and R. J. Hemley, *Science* **293**, 272 (2001).
- [14] D. N. Sanz, P. Loubeyre, and M. Mezouar, *Phys. Rev. Lett.* **89**, 245501 (2002).
- [15] J. S. Tse, *Nature (London)* **457**, 800 (2009).
- [16] M. Sakai, *Acta Metall. Mater.* **41**, 1751 (1993).
- [17] R. F. Zhang, D. Legut, R. Niewa, A. S. Argon, and S. Veprek, *Phys. Rev. B* **82**, 104104 (2010).
- [18] R. F. Zhang, D. Legut, Z. H. Fu, S. Veprek, Q. F. Zhang, and H. K. Mao, *Phys. Rev. B* **92**, 104107 (2015).

- [19] B. Joós, Q. Ren, and M. S. Duesbery, *Phys. Rev. B* **50**, 5890 (1994).
- [20] S. H. Zhang, I. J. Beyerlein, D. Legut, Z. H. Fu, Z. Zhang, S. L. Shang, Z. K. Liu, T. C. Germann, and R. F. Zhang, *Phys. Rev. B* **95**, 224106 (2017).
- [21] H. F. Rizzo, W. C. Simmons, and H. O. Bielstein, *J. Electrochem. Soc.* **109**, 1079 (1962).
- [22] D. W. He, Y. S. Zhao, L. Daemen, J. Qian, T. D. Shen, and T. W. Zerda, *Appl. Phys. Lett.* **81**, 643 (2002).
- [23] H. Itoh, R. Yamamoto, and H. Iwahara, *J. Am. Ceram. Soc.* **83**, 501 (2000).
- [24] R. Sasai, H. Fukatsu, T. Kojima, and H. Itoh, *J. Mater. Sci.* **36**, 5339 (2001).
- [25] M. Herrmann, I. Sigalas, M. Thiele, M. M. Müller, H. J. Kleebe, and A. Michaelis, *Int. J. Refract. Met. Hard Mat.* **39**, 53 (2013).
- [26] See Supplemental Material at <http://link.aps.org/supplemental/10.1103/PhysRevMaterials.2.123602> for details of the methods of experiment, first-principles calculation, ideal strength model, ideal cleavage stress and *ab initio* informed P-N model, as well as the average measured H_v for monocrystalline γ -B₂₈ under different loads.
- [27] These two specific planes are chosen because they correspond to the weakest slip system, i.e., (001)[010], and the weakest tensile direction, i.e., [011], respectively.
- [28] D. M. Clatterbuck, C. R. Krenn, M. L. Cohen, and J. W. Morris, Jr., *Phys. Rev. Lett.* **91**, 135501 (2003).
- [29] S. M.-M. Dubois, G. M. Rignanese, T. Pardoen, and J. C. Charlier, *Phys. Rev. B* **74**, 235203 (2006).
- [30] R. F. Zhang, S. Veprek, and A. S. Argon, *Phys. Rev. B* **77**, 172103 (2008).
- [31] D. Roundy and M. L. Cohen, *Phys. Rev. B* **64**, 212103 (2001).
- [32] P. Lazar, X. Q. Chen, and R. Podlucky, *Phys. Rev. B* **80**, 012103 (2009).
- [33] S. F. Wang, H. L. Zhang, X. Z. Wu, and R. P. Liu, *J. Phys.: Condens. Matter* **22**, 055801 (2010).
- [34] J. N. Wang, *Mater. Sci. and Eng. A* **206**, 259 (1996).
- [35] D. M. Teter, *MRS Bull.* **23**, 22 (1998).
- [36] S. Veprek, R. F. Zhang, and A. S. Argon, *J. Superhard Mater.* **33**, 409 (2011).